

## Magnetization of erbium in the ordered and paramagnetic phases

Sergio Gama and Mário E. Fóglio

*Universidade Estadual de Campinas, Instituto de Física "Gleb Wataghin," Cidade Universitária, Barão Geraldo, 13081 Campinas, São Paulo, Brazil*

(Received 17 September 1986; revised manuscript received 24 July 1987)

We present measurements of Er magnetization in the paramagnetic and ordered phases. Our values agree with those already published by other authors, but a small anomaly in the basal-plane magnetization was also noted in the conical phase. By extension of the theoretical model of Jensen, it was possible to reproduce the characteristics of the paramagnetic and sinusoidal arrangements with a single set of parameters. Another set of parameters was necessary to describe the conical and low-temperature antiferromagnetic phases. The model provides a possible explanation for the experimental anomaly in the conical phase, and suggests a different arrangement of spins for the low-temperature antiferromagnetic phase.

### I. INTRODUCTION

The present work is part of a plan for studying the strong magnetoelastic effects that are exhibited by erbium. Our objective was to measure the magnetization and the elastic constants of erbium on the same sample in order to have a reliable basis for correlating the two quantities. In this paper we present measurements of the magnetization of single-crystal erbium as a function of temperature and magnetic field, and we provide a model to describe these results. The measurements of the elastic constants as well as their description within the framework of the model presented here will be discussed in another paper.

It is well established<sup>1,2</sup> that erbium is a hexagonal metal that presents several magnetic phases at zero applied magnetic field: down to 85 K it is paramagnetic, from 85 K down to 53 K it is antiferromagnetic, having the spins confined to the  $c$  axis and sinusoidally modulated in amplitude with a period of approximately seven layers. From 53 K down to 18 K it is still antiferromagnetic, but with spin components in the basal plane forming a helix, and with the  $c$  axis ordering "squaring up" as the temperature is lowered. From 18 K down, it is a conical ferromagnet with a period of 8.4 layers for the basal-plane helix. After this paper was submitted, we were made aware of a very recent neutron and x-ray diffraction work of Gibbs *et al.*<sup>3</sup> that shows the existence of both commensurate and incommensurate spin structures. Through the measurement of the wave vector  $\tau_m$  of the  $c$ -axis spin modulation, Gibbs *et al.* were able to detect a series of first-order transitions between the two types of structures in the range from 53 to 18 K, and observed that the value of  $\tau_m$  (in units of  $c^*$ ) would lock at rational values (commensurate phases) for several intervals of temperature. Above 26.5 K the commensurate phases are separated by incommensurate ones, while below 26.5 K only commensurate phases occur. In the conical ferromagnet phase,  $\tau_m = \frac{5}{21}$ , and the lowest temperature antiferromagnetic phase has  $\tau_m = \frac{1}{4}$  in the inter-

val 18–23 K. Gibbs *et al.*<sup>3</sup> were able to make a very clear interpretation of their results by employing the concept of spin slip (spin discommensuration).<sup>4</sup> The model we present suggests, for the antiferromagnetic phase between 53 and 18 K, an arrangement of spins that is alternative to that proposed by Jensen.<sup>5</sup> The fine details of the magnetic structure observed by Gibbs *et al.*<sup>3</sup> in this temperature interval are not described by our model, because we assume from the start a periodicity along the  $c$  axis of seven or eight layers only. Nevertheless, we believe that the gross features of the dependence of the magnetic structures with the applied field that we calculate are essentially correct, even in the 18–53 K interval. We shall discuss in another section a natural extension of our model that would incorporate the structural details that are now available.

As the magnetization and elastic constants were measured on the same sample, its shape was not optimal for magnetization measurements. The shape was an irregular cylinder with its axis along the  $a$  direction, and having two sets of plane and parallel faces which were cut perpendicular to the  $a$  and  $c$  axis, respectively, of the hexagonal crystal. Although no attempt was made to correct the data for demagnetization effects, our values are in close qualitative agreement with those previously published.<sup>1,2,6,7</sup> We believe that the shape of our samples was the main reason for the minor discrepancies between our data and those in the literature.<sup>1,2,6</sup> An additional possible source is the fact that magnetization results depend sensitively on the sample preparation.

To describe the magnetic behavior of erbium, we have employed a model that follows closely the molecular-field treatment proposed by Jensen.<sup>5</sup> Some of the parameters in our model were those suggested by Jensen or found in the literature,<sup>1,2</sup> and the remaining ones were adjusted to reproduce the different magnetic structures of Er. As noted by Jensen,<sup>5</sup> the model offers an alternative structure for the low-temperature antiferromagnetic phase. We have also found that the model predicts a new sequence of magnetic structures in the conical ar-

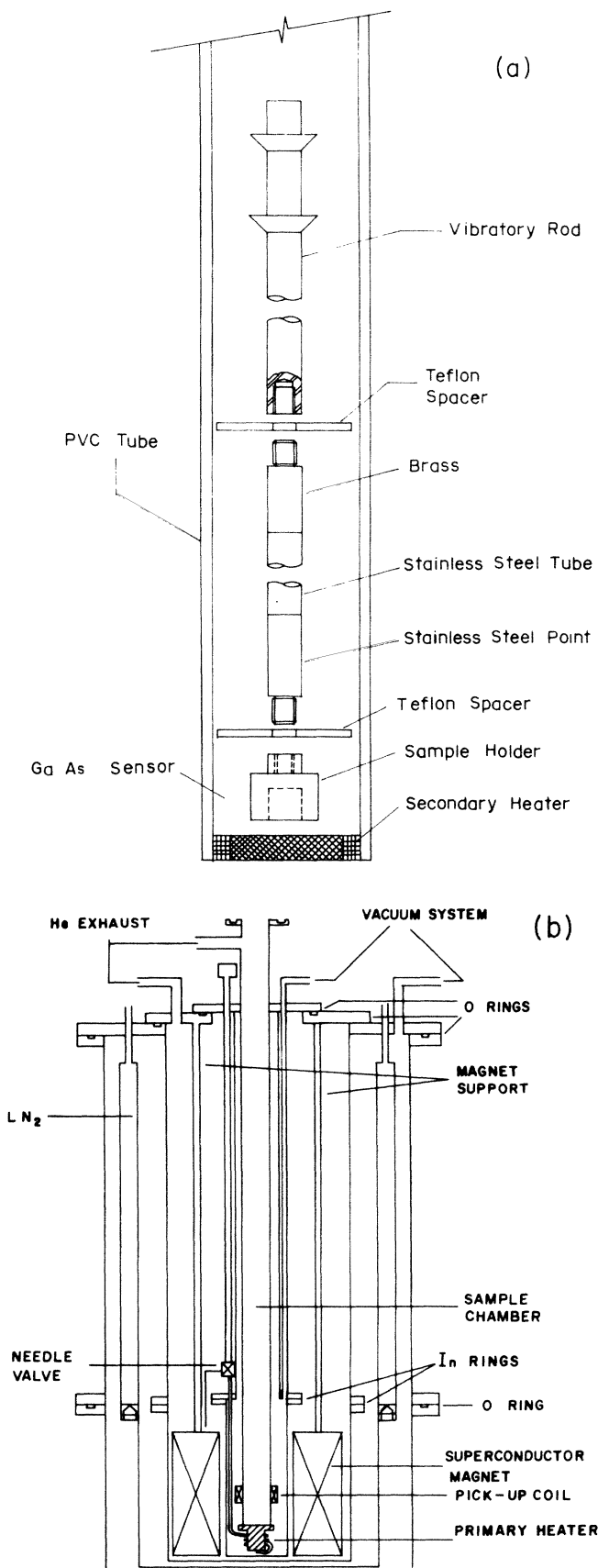


FIG. 1. (a) Exploded view of magnetometer sample holder; (b) cryogenic system.

range when a magnetic field is increased along the basal plane. The transition fields in this new sequence are compatible with those experimentally observed.

In Sec. II we describe the sample, the experimental techniques, and the equipment employed, while in Sec. III we give the results of our measurements. A theoretical model and the approximations we employ for Er metal are presented in Sec. IV, and the numerical procedures are given in Sec. V. In Sec. VI a fairly good description of both our experimental results, and those found in the literature, was obtained with two sets of parameters: one for high, and the other for low temperatures. A summary and the conclusions are presented in Sec. VII.

## II. MATERIALS AND METHODS

The Er sample was a single crystal obtained from Metals Research Company with a claimed purity of 99.9%. The sample was in the form of an irregular cylinder, with two pairs of plane and parallel faces, with separations of 0.87 cm in the  $a$  direction and 0.59 cm in the  $c$  direction. The cuts were done in an electroerosion machine, and were oriented by Laue back reflection. The lack of parallelism is estimated to be less than  $0.03^\circ$  and the orthogonality to the crystallographic axis is within  $2^\circ$ . The mass of the sample was 3.14 g.

The sample magnetization was measured with a vibrating sample magnetometer from Princeton Applied Research, model 155. The pickup coils were wound in the inner walls of the sample chamber of the cryostat used, in the manner indicated in Fig. 1(b). This set of coils was calibrated using a cylindrical sample of high purity Ni at 4.2 K. The sample holder is described in Fig. 1(a), where we should note that the extremity of the vibrating rod was made of stainless steel. This material was chosen so that it could stand the high torques that appear in the sample when it is in an ordered state and it is submitted to high magnetic fields in the hard directions. A test showed that the influence of the metallic point vibrating together with the sample could be neglected.

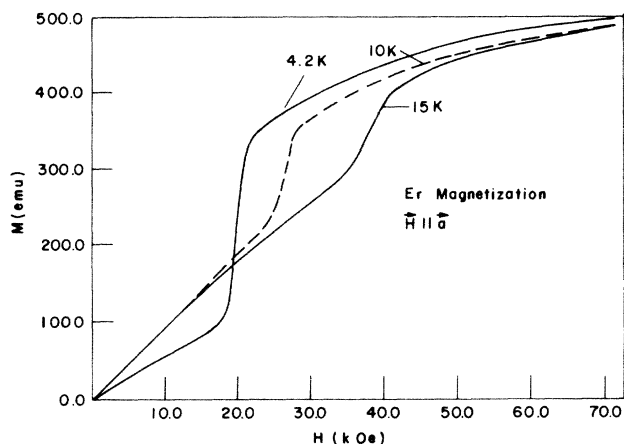


FIG. 2.  $a$ -axis Er magnetization in the conical phase.

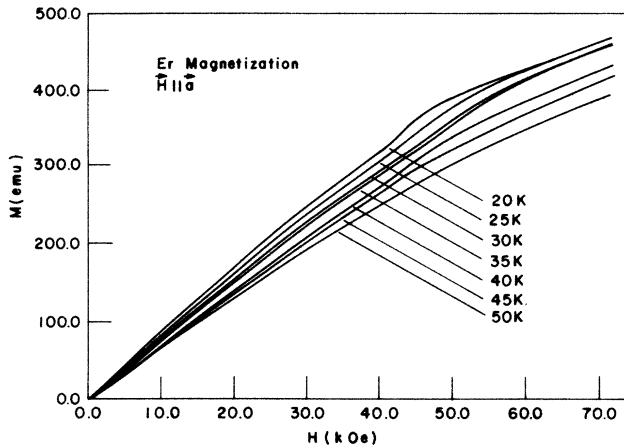


FIG. 3.  $a$ -axis Er magnetization in the antiferromagnetic phase between 18 and 53 K.

The cryogenic system (Oxford Company) is described in Fig. 1(b). It consisted of a liquid- $N_2$  jacket and a liquid-helium chamber that housed the superconducting magnet. The magnet was calibrated in the factory with a proton-resonance probe and allowed high homogeneity fields up to 7.2 T. The sample chamber was introduced in the liquid-helium chamber, which was vacuum isolated and received helium from the main reservoir through a needle valve. This helium was forced into the sample chamber by overpressurizing the helium chamber, and was used to control the temperature of the sample. The temperature controller was built in our laboratory. It was of the proportional type, and used a GaAs diode as a temperature sensor. This sensor was placed in the wall of the sample holder, very near the sample, and was calibrated against a Cu-Constantan couple. Typically the temperature could be maintained constant within 0.01 K, but its absolute value could only be determined within 0.1 K. Measurements at different dates of the magnetization as a function of applied field for a given temperature showed that the overall reproducibility for

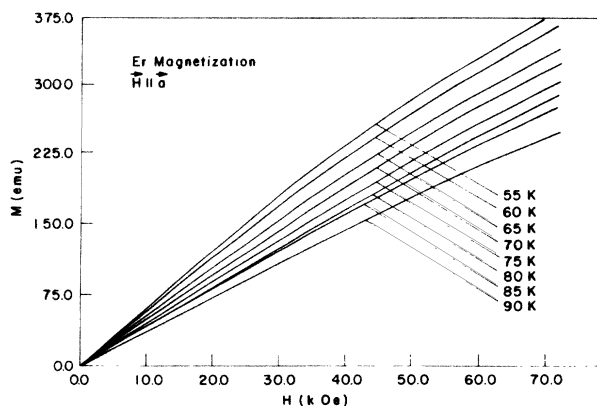


FIG. 4.  $a$ -axis Er magnetization in the sinusoidal and paramagnetic phases.

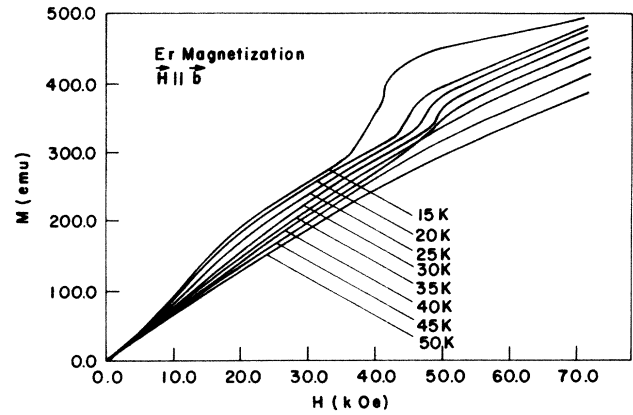


FIG. 5.  $b$ -axis Er magnetization in the conical and antiferromagnetic phase between 18 and 53 K.

the magnetization data in the entire temperature range was within 2%.

### III. EXPERIMENTAL RESULTS

In this work we have only measured the magnetization in the direction of the applied field. The  $a$ -axis magnetization as a function of applied field is shown in Figs. 2–4, and the  $b$ -axis magnetization in Figs. 5 and 6. Figure 2, which displays the  $a$ -axis magnetization for the conical ferromagnetic phase shows a phase transformation whose critical field is a function of temperature. This does not agree with the data of Feron *et al.*,<sup>6</sup> which display this transition at the same critical field for all the temperatures of this phase. The values calculated with our theoretical model indicate that these critical fields are also temperature dependent. Figure 5 clearly shows a small anomaly in the magnetization of the low-temperature ferromagnetic phase at small values of the applied field (about 10 kOe). This anomaly is also present in the data of Feron *et al.*,<sup>6</sup> but no discussion about its origin was given.<sup>1,2</sup> At higher fields we have a

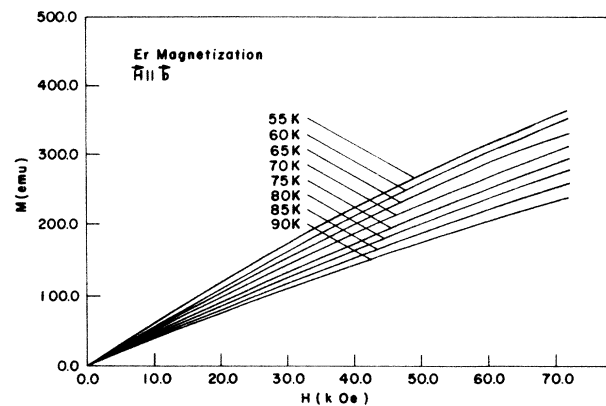


FIG. 6.  $b$ -axis Er magnetization in the sinusoidal and paramagnetic phases.

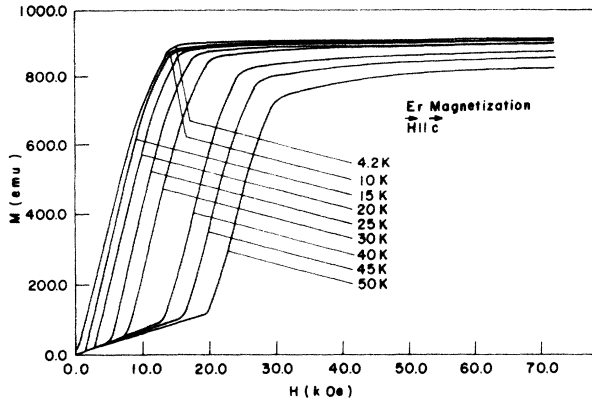


FIG. 7.  $c$ -axis Er magnetization in the conical phase (up to 18 K) and in the low-temperature antiferromagnetic phase (between 18 and 53 K).

second transition which is really a sequence of two consecutive transitions, as clearly shown by the 15-K curve in Fig. 5. This phenomenon is more clearly shown for the same configuration in the data of Feron *et al.*<sup>6</sup> because their samples had a more favorable geometry for the magnetization measurements. This second transition is ascribed<sup>1</sup> to the collapse of the basal-plane helix to a fan structure around the applied field. It should also be noted that the magnetization curves for the sinusoidal antiferromagnetic phase are very similar to the paramagnetic ones (cf. Figs. 4 and 6).

Figures 7 and 8 show the  $c$ -axis magnetization, and the transition to a ferromagnetic state is clearly shown in the antiferromagnetic phase. At 27, 34, and 52.4 K, the susceptibility of polycrystalline Er shows anomalies that have been connected by Gibbs *et al.*<sup>3</sup> to the existence of a net magnetization along the  $c$  axis in the temperature intervals in which  $\tau_m = \frac{7}{7}$ ,  $\frac{4}{15}$ , and  $\frac{6}{23}$ . Our measurements were performed at constant temperature, and included two values (25 and 50 K) that were inside one of those intervals, but we did not observe any appreciable magnetization at zero field. We do not feel that

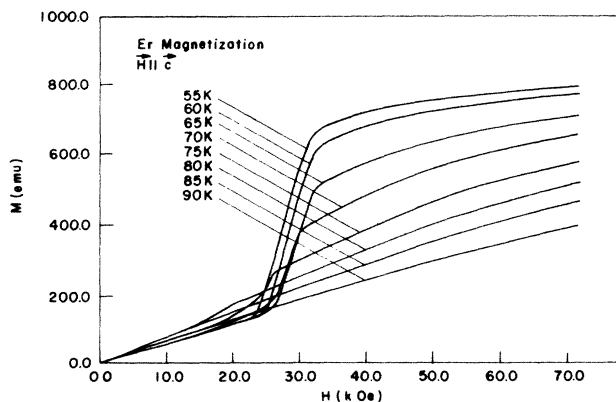


FIG. 8.  $c$ -axis Er magnetization in the sinusoidal and paramagnetic phases.

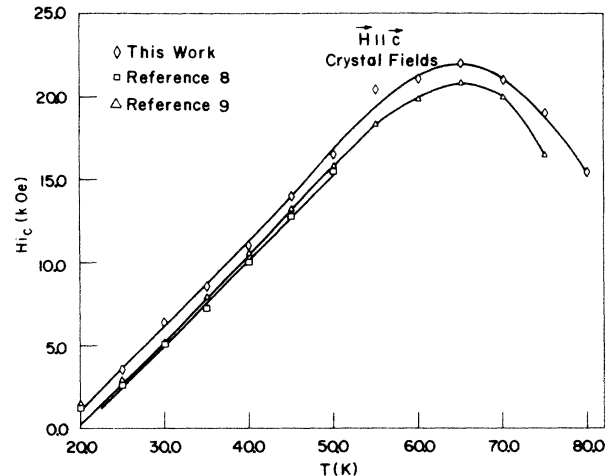


FIG. 9. Er critical internal fields in the antiferromagnetic range. Our values are presented together with those of Refs. 5 and 6.

this result is conclusive, because we did not perform any measurements at decreasing field strength that could rule out the effect of magnetic domains. In Fig. 9 the internal fields we measured at this transition are compared with those determined by Rhyne *et al.*<sup>8</sup> and Flippen,<sup>9</sup> and a good agreement is observed. To determine the internal fields, we employed a demagnetization factor obtained by trial and error, so that the 20-K curve, as a function of the internal field, was vertical at the transition point.

#### IV. THE THEORETICAL MODEL

Jensen<sup>5</sup> proposed a molecular-field model that would be consistent with the available neutron diffraction data for Er. From the data of Nicklow *et al.*<sup>10</sup> he concluded<sup>11</sup> that the two-ion anisotropy should be included in the description of the system. The model Hamiltonian he proposed was

$$\mathcal{H} = \mathcal{H}_{\text{ex}} + \mathcal{H}_{\text{Ze}} + \mathcal{H}_{\text{CF}}. \quad (1)$$

The first term describes the exchange interaction:

$$\mathcal{H}_{\text{ex}} = -\frac{1}{2} \sum_{i \neq j} \left\{ \mathcal{J}(i, j) \mathbf{J}_i \cdot \mathbf{J}_j - \frac{1}{2} \mathcal{H}_{22}(i, j) \frac{1}{8J_1^2} [(J_i^+ J_j^-)^2 + (J_i^- J_j^+)^2] \right\} \quad (2)$$

where  $\mathbf{J}_i$  is the total angular momentum of the  $i$ th ion and we choose the crystal  $c$  axis as the  $z$  axis. We also employ the abbreviation

$$J_n = (J - \frac{1}{2})(J - 1) \cdots (J - \frac{n}{2}).$$

The term

$$\mathcal{H}_{\text{Ze}} = - \sum_i g \mu_B \mathbf{H} \cdot \mathbf{J}_i \quad (3)$$

is the Zeeman interaction and

$$\mathcal{H}_{\text{CF}} = \sum_i [B_{20}O_{20}(i) + B_{40}O_{40}(i) + B_{60}O_{60}(i) + B_{66}O_{66}(i)] \quad (4)$$

is the crystal-field Hamiltonian, where the  $O_{lm}(i)$  are Stevens operators associated to the  $i$ th ion, as defined by Lindgard and Danielsen.<sup>12</sup> To reduce the problem to a system of linked one-ion problems, we employ the molecular-field approximation. All the ions in a layer (perpendicular to the  $c$  axis) are ferromagnetically coupled, and the system can be described, assuming that  $\langle \mathbf{J}_i \rangle$  is the same for all the ions in the same layer. The problem is then reduced to the study of a single ion in each layer described by an effective Hamiltonian

$$\mathcal{H}_{\text{eff}}^{(i)} = - \sum_j \{ \mathcal{J}_j \cdot \mathbf{J}_i - \mathcal{H}_j^+ (J_i^-)^2 - \mathcal{H}_j^- (J_i^+)^2 - \frac{1}{2} [ \mathcal{J}_j \cdot \langle \mathbf{J}_i \rangle - \mathcal{H}_j^+ \langle (J_i^-)^2 \rangle - \mathcal{H}_j^- \langle (J_i^+)^2 \rangle ] \}, \quad (5)$$

where we have introduced the molecular fields

$$\mathcal{J}_j^\alpha = \sum_i \mathcal{J}(i,j) \langle J_i^\alpha \rangle = \sum_{m=-6}^6 J_{|m|} \langle J_{j+m}^\alpha \rangle, \quad (6a)$$

$$\mathcal{H}_j^\pm = \frac{1}{8J_1^2} \sum_{m=-5}^5 K_{|m|} \langle (J_{j+m}^\pm)^2 \rangle, \quad (6b)$$

$$\alpha = x, y, \text{ or } z,$$

and the  $J_{|m|}$  and  $K_{|m|}$  characterize the exchange interaction between one ion in the layer  $j$  with all those in the layer  $j \pm m$ .<sup>5</sup>

The values of the parameters  $J_m$ ,  $K_m$ , and  $B_{lm}$  have been determined by Jensen using neutron diffraction data, the Néel temperatures, and magnetization data.<sup>5</sup> With this set of parameters,<sup>11,13</sup> however, we noticed some discrepancies with the experimental data.

(1) The paramagnetic Curie temperatures are not reproduced.

(2) The cone angle in the conical ferromagnetic phase does not agree with the experimental value.

(3) The spin arrangement of the antiferromagnetic phase between 53 K and 18 K has lower free energy than that of the cone, even down to 0 K.

To overcome these difficulties we included in the Hamiltonian a second anisotropy term of the form

$$\mathcal{H}_{\text{an}} = -\frac{1}{2} \sum_{i,j} \mathcal{H}(i,j) J_{iz} J_{jz}, \quad (7)$$

as was already suggested by Jensen.<sup>5</sup> The neutron dispersion relations would be altered by the introduction of this general two-ion term, and one should accordingly modify the  $J_m$ . Instead of following this procedure, we

noticed that the dispersion relations are not altered when the  $\mathcal{H}(i,j)$  are the same for all pairs  $i,j$ , and we then employed

$$\mathcal{H}_{\text{an}} = -\frac{\Delta}{2} \sum_{i,j} J_{iz} J_{jz} \quad (8)$$

as the extra term, without modifying the  $J_m$  and  $K_m$  parameters proposed by Jensen.<sup>11</sup> The main effect of  $\mathcal{H}_{\text{an}}$  is to introduce an exchange anisotropy along the  $c$  axis, and in our mean-field approximation it only adds a constant contribution to the  $z$  component of the molecular field. It is then clear that this term would serve to stabilize the cone structure against the antiferromagnetic one. The inclusion of the full term<sup>5</sup> would imply a large increase in the number of parameters to be determined, making the reevaluation of the  $J_m$  and  $K_m$  parameters necessary also. We feel that this large increase in computational difficulty would not really improve our understanding of the problem very much, and we decided to employ the simpler form of  $\mathcal{H}_{\text{an}}$  given in Eq. (8). For the values of  $\Delta$  used in the calculation, the  $\mathcal{H}_{\text{an}}$  did not result in any substantial change of the magnetic structures, but only in a modification of their relative stabilities.

Within our model we could not find a unique set of parameters  $\Delta$ ,  $B_{20}$ , and  $B_{40}$  that describes the magnetization in the whole range of temperature, but this could be achieved with two sets of values, one for the paramagnetic and sinusoidal arrangements, and the other for the conical and the low-temperature antiferromagnetic phase. The values we employed were not very different from those proposed by Jensen. In the low-temperature range we adjusted  $\Delta$  so that the antiferromagnetic and the conical structures had the same free energy at 18 K. With this device the phase with lower free energy below 18 K was the conical, and above 18 K it was the antiferromagnetic phase. The value of  $B_{20}$  was maintained because of its importance in the determination of the Néel temperatures, and we adjusted the value of the cone angle using  $B_{40}$ , which has little effect on the Néel temperatures.

In the high-temperature range we maintained the value of  $B_{40}$  obtained at low temperature and adjusted, simultaneously,  $\Delta$  and  $B_{20}$  to reproduce the paramagnetic Curie temperatures. The two sets of values are given in Table I.

The two values of  $\Delta$  in Table I are fairly small compared to the average values of the  $J_m$  and  $K_m$ , so that  $\mathcal{H}_{\text{an}}$  is only a moderate correction to the Hamiltonian of the system. The fact that different values of  $\Delta$  are used at high and low  $T$  is not just because of the imperfection of the Hamiltonian employed. We should point out two other sources of this problem. One is that the mean-field theory is not completely satisfactory at low temperature, because of the neglect of low-energy excitations that distort the values of the thermodynamic quantities, while giving an overall behavior that is reasonable. The other possible source of the discrepancy is that we assume that all the remaining parameters are independent with  $T$ , although one should certainly expect some variations due to the changes in the lattice size.

TABLE I. Values of the parameters used in the molecular-field calculations.  $B_{lm}$  parameters in K/ion units.

$m$	$J_m$	$K_m$		High $T$	Low $T$
0	10.58	0	$B_{20}$	-2.0	-1.27
1	3.71	-1.739	$B_{40}$	0.033	0.033
2	-1.09	-1.677	$B_{60}$	0.003	0.003
3	-0.15	-1.955	$B_{66}$	-0.020	-0.020
4	-0.68	0.838	$\Delta$	0.060	0.293
5	-0.67	-2.534			
6	-0.15				

## V. NUMERICAL PROCEDURE

Given a set of model parameters, the effective Hamiltonian  $\mathcal{H}_i$  for the  $i$ th layer is a function of the expectation values  $\langle O \rangle_j$  of several operators  $O$  calculated for the  $j$ th layer. To obtain  $\langle O \rangle_j$  we need the solution of the eigenvalue problem

$$\mathcal{H}_j |v, j\rangle = E_j^v |v, j\rangle \quad (9)$$

associated to the  $j$ th layer, and by definition,

$$\langle O \rangle_j = \sum_v \exp(-E_j^v/kT) \langle v, j | O | v, j \rangle / Z_j, \quad (10)$$

where

$$Z_j = \sum_v \exp(-E_j^v/kT). \quad (11)$$

We only consider the  $(2J+1)$ -dimensional space associated with the ground multiplet of an ion in each layer, and a different matrix of order  $2J+1$  has then to be diagonalized for each layer. Because of the exchange terms, the effective  $\mathcal{H}_i$  depends on the averages  $\langle J^\alpha \rangle_j$  and  $\langle (J^\pm)^2 \rangle_j$  associated with the six nearest layers, i.e., with  $|j-i| < 6$  (cf. Table I), and the problem must be solved self-consistently. One assumes starting values for the  $\langle J^\alpha \rangle_j$  in all the layers (only periods of seven or eight layers are considered in the present work) and, with them, all the required effective  $\mathcal{H}_i$  are constructed. These  $\mathcal{H}_i$  are diagonalized numerically, new averages  $\langle J^\alpha \rangle_j$  and  $\langle (J^\pm)^2 \rangle_j$  are then calculated with Eq. (9), and new effective  $\mathcal{H}_i$  are constructed. The procedure is repeated until self-consistency is achieved. Within this model, the free energy of the system is the sum of all the single-ion free energies

$$F_i = -kT \ln Z_i. \quad (12)$$

To reduce the computation time to manageable proportions we made the calculation with a system of ions with spin  $S=3$  rather than with the  $J=7.5$  of Er. This choice was made because 3 is the smallest value for which all the matrix elements of the crystal-field operators  $O_{lm}$  are not automatically zero due to the triangle rule. It was necessary to renormalize all the parameters, and we multiplied the two-ion parameters by  $S(S+1)/S'(S'+1)$ , the crystal-field ones by  $(S/S')^l$ , with  $l=2, 4, 6$ , and the Zeeman and one-ion exchange by  $S/S'$ , where  $S=7.5$ .

## VI. THE RESULTS OF THE MODEL AND THE EXPERIMENTAL VALUES

### A. Paramagnetic phase

The magnetization has been calculated for fields up to 500 kOe along the  $a$  and  $c$  axes for temperatures of 90, 100, 110, and 120 K. The agreement with experimental data is good, as revealed by the calculated paramagnetic Curie temperatures  $\theta_{||}=60.5$  K and  $\theta_{\perp}=32.4$  K, as compared to the experimental ones,  $\theta_{||}=61.7$  K and  $\theta_{\perp}=32.5$  K.

### B. Sinusoidal phase

#### 1. Field along the $a$ axis

The temperature 65 K was chosen as representative for this spin arrangement and, according to the experiment, a seven-layer period was used for the spin arrangement. With the field applied along the  $a$  axis, the original  $z$ -sinusoidal arrangement distorts into a fan centered on the field direction, such that the angle of the fan decreases as the strength of the field increases. According to the model, this fan transforms continuously into a ferromagnet at a field of 160 kOe, and this transition appears in the magnetization curve as a change of slope. Up to 70 kOe the magnetization behavior is similar to that of the paramagnet, as is indicated by experiment. The model gives a susceptibility  $\sigma/H = 5.71 \times 10^{-6}$  Oe $^{-1}$ , while our experimental value is  $5.14 \times 10^{-6}$  Oe $^{-1}$ .

#### 2. Field along the $c$ axis

For this direction of the field an antiferromagnetic-ferromagnetic transition is expected. The determination of the transition field presents some difficulties, because there might be several self-consistent solutions for the same field, and the solution obtained in each calculation depends on the starting values for the operator averages. The procedure adopted was to start from a field in which the low-field phase is still stable, and use the corresponding self-consistent solution to calculate the starting values for a field with a small increment. A new self-consistent solution is obtained, and the procedure is repeated until at a certain field a different phase is obtained as the self-consistent solution. The process is then inverted, decreasing the field until the low-field

phase is obtained again. In this interval, two self-consistent solutions are obtained for each field (one when the field increases and the other when the field decreases), and the crossing point of the free energies gives the transition field.

At 65 K the model predicts a ferromagnetic phase transition at a field of 26 kOe, the magnetization curve presenting a jump at this field of magnitude  $\Delta\sigma=0.33$ . Our experimental values are  $H=22.4$  kOe and  $\Delta\sigma=0.41$ .

### C. Antiferromagnetic structure between 18 and 53 K

We chose 40 K as the temperature representative of this phase, and a period of eight layers was used in the calculation. We should point out that the experimental periodicity of the spin arrangement<sup>2,14,15</sup> along the  $c$  axis changes continuously with temperature. The use of an exact periodicity of seven or eight layers in our model should only be considered as an approximation that makes the numerical calculation possible. In the present range of temperature all the spin arrangements with seven layers presented a net magnetization along the  $c$  axis, i.e., a ferrimagnetic rather than an antiferromagnetic structure, and this behavior was also obtained with Jensen's seven-layer arrangement.<sup>5</sup> The eight-layer structure we discuss below is the one with lowest free energy from all those obtained with seven- and with eight-layer periodicity. Previous interpretations of the neutron diffraction experiments<sup>14,15</sup> predicted an antiferromagnetic structure with a  $z$  component of magnetization that is sinusoidal at 53 K, and that becomes progressively squared as the temperature decreases. To obtain this type of modulation the higher Fourier harmonics became more important at lower temperatures. In the basal plane the projection of the magnetization of the different layers form a helix, with a wave vector that is the same as the fundamental harmonic of the  $c$ -axis modulation. Based on his analysis, Jensen concluded<sup>5</sup> that this structure can also be described by a helix of spins practically confined to the  $xz$  plane, and that this helix is consistent with the spin-wave dispersion relations determined experimentally.<sup>11</sup> Jensen's Hamiltonian, however, gives origin to other structures as well, and it turns out that a helix of spins confined in a plane perpendicular to the basal plane but at  $45^\circ$  from the  $a$  axis is more stable than the structure proposed by Jensen. This structure, predicted by our model, gives better accord with both Feron's and our own measurements. In the two cases, both the  $a$ - and  $b$ -axis magnetization change with field in a similar way, and one would expect a rather different behavior with Jensen's structure. The temperature we considered (40 K) corresponds to the region in which Gibbs *et al.*<sup>3</sup> observe commensurate phases separated by incommensurate ones, and is close to the phase locked at  $\tau_m = \frac{3}{11}$ . Spin structures with seven-layer periodicity and with spin slips similar to those described by Gibbs *et al.*<sup>3</sup> are also present at 40 K in our model, but all had higher free energies than the eight-layer helix described above. A periodicity of 22 layers ( $\tau_m = \frac{3}{11}$ ) would be a better description of the system,

and a simple extension of our model following the method discussed in Ref. 4 would give better results. One should repeat the calculation with several periodicities  $N$  (e.g.,  $N=21, 22, 23$  to study  $\tau_m = \frac{3}{11}$ ) and take the structure with minimum free energy. The next step would be to choose the model parameters so that the experimental  $\tau_m$  would be obtained in the correct intervals of  $T$ . The computation time required for this project would increase very much over that of our original model, and we have not attempted that calculation.

#### 1. Field along the $a$ axis

Our model predicts that for low fields, close to 4 kOe, the spin components leave the plane they occupy at zero field (at  $45^\circ$  from the  $a$  axis) and form a complex fan around the field direction. At 8 kOe all the  $x$  components point in the same direction, though oscillating in amplitude, and we have an antiferromagnetic fan centered around the field direction. This fan transforms continuously into a fan confined to the plane  $xz$ , and this transformation is completed around 70 kOe. This fan changes continuously with the field until complete ferromagnetic alignment is reached at 260 kOe. Figure 10 shows these structures and the magnetization curve schematically.

The magnetization data found in the literature,<sup>1,6</sup> as well as our own data, do not show any clear indication of any abrupt transition, and this is in accord with our model. Unfortunately, there are no experiments of neutron diffraction at a fixed temperature with different magnetic fields that would reveal the different structures in this antiferromagnetic phase, as a function of magnetic field. That type of measurement was performed by Rhyne and Pickart<sup>16</sup> for the conical phase at 4.2 K.

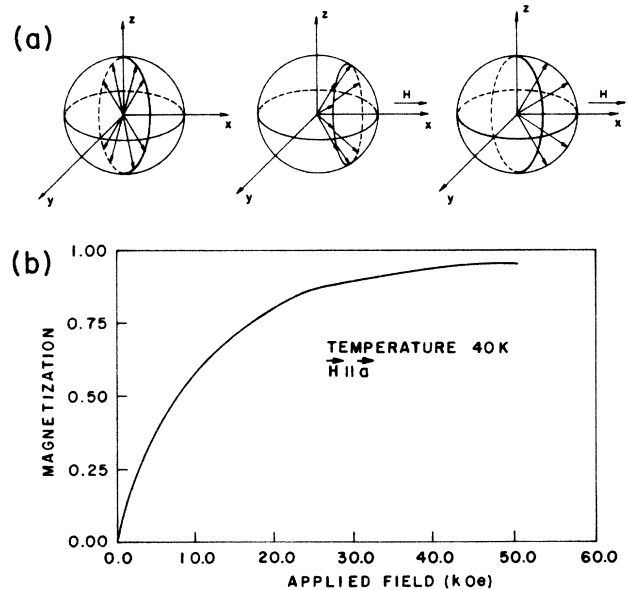


FIG. 10. (a) Sequence of spin configurations induced by a magnetic field applied along the  $a$  axis for the antiferromagnetic helix, according to the theoretical model (see text), (b) magnetization curve for the same sequence.

## 2. Field along the $c$ axis

The model predicts a two-step transition to ferromagnetism. In the first step at 14 kOe, two layers change the direction of the  $z$  component of magnetization, and in the second step at 26 kOe the magnetization of all the layers becomes parallel to the  $z$  axis. The spin arrangement at 18 kOe and the magnetization curves are represented in Fig. 11. Both the magnetization data in the literature and our own results seem to indicate a single-step transition that starts at lower fields, namely, from 10–12 kOe at 40 K. However, magnetostriction measurements in this phase, at this temperature, and with the field applied parallel to the  $c$  axis,<sup>17</sup> as well as our own measurements of the elastic constants  $C_{11}$  and  $C_{33}$  as a function of the applied field, suggest the presence of a transition at higher fields than those observed in the magnetization measurements. The curve of deformation versus field<sup>17</sup> reveals an abrupt change in the  $c$  strains at 18 kOe with a sharp peak at the end of the transition. A similar behavior is observed for the elastic constants  $C_{11}$  and  $C_{33}$  as shown in Fig. 12, and one should particularly note that  $C_{33}$  shows a small peak at 19 kOe followed by a sharp increase starting at 20 kOe. It is to be noted that when there is an abrupt change of magnetization in a transition, the magnetostriction and the elastic constants follow closely the magnetization behavior.<sup>17,18</sup> The behavior of the magnetostriction and of the elastic constants gives, then, some credibility to the two-step transition predicted by our model in this antiferromagnetic phase. Nevertheless, in view of the results of Gibbs *et al.*,<sup>3</sup> we believe that there is only one transition as indicated by the experimental magnetization curve. Note that, although the magnetization starts to change at 12 kOe, it only reaches a plateau at approximately 24 kOe, and we believe that this gradual change is due to demagnetization effects, because the shape of our sample is not ellipsoidal. The simple transition would really occur close to 18 kOe, as indicated by the elastic properties. We attribute the calculated two-jump transition to our forcing on the model an eight-layer periodicity, rather than the one close to 22 layers, that corresponds to the  $\tau_m = \frac{3}{11}$  observed near this temperature. A larger and variable periodicity would describe much better the incommensurate phases that are close to this temperature.

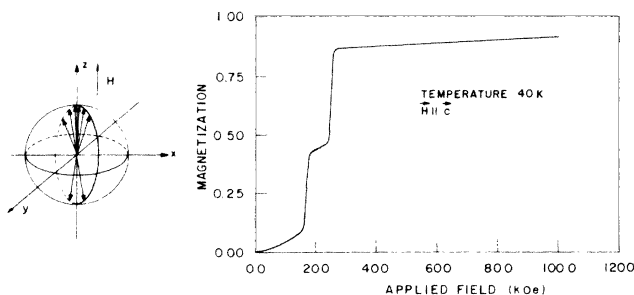


FIG. 11. (a) Spin configuration of the antiferromagnetic helix for a magnetic field applied along the  $c$  axis after the first step of the induced transition, (b) magnetization curve for field applied along the  $c$  axis, according to the model (see text).

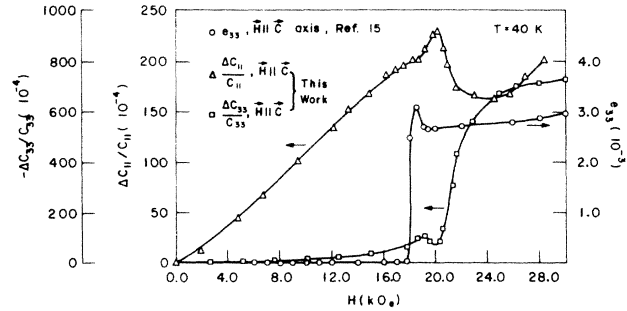


FIG. 12. The  $c$ -axis magnetostriction and the  $C_{11}$  and  $C_{33}$  elastic constants at 50 K, for a field applied along the  $c$  axis.

## D. Conical phase

### 1. Field along the $a$ axis

We chose 10 K as the representative temperature for the conical phase and used, as indicated by experiment,<sup>1</sup> a period of eight layers for the spin arrangement. As the field is increased, our model shows that the cone distorts so that its axis makes an angle with the  $c$  axis, and the basal-plane helix of spins presents a net ferromagnetic component. This distorted cone transforms, at a field of 12 kOe, into a fan centered around the field direction. At 56 kOe this fan becomes a ferromagnet with the angle  $\theta = 32.5^\circ$ , and as the field increases the angle  $\theta$  decreases until complete ferromagnetic alignment along the  $a$  axis is achieved at a field of 300 kOe. This sequence of structures can be imagined as a progressive distortion of the original cone arrangement and follows closely the sequence of structures suggested by the work of Kitano and Nagamiya.<sup>19</sup> Nevertheless, at a field close to 12 kOe, the antiferromagnetic structures described in Sec. VI C become more stable than the ones derived from the cone. This situation persists up to 26 kOe, when the structure derived from the cone becomes again more stable. The existence of this effect should be clearly demonstrated by measuring the  $c$  component of the magnetization, which is zero in the phase predicted by our model, but we have found no reports of this type of measurement in Er.

The induced sequence of magnetic structures in our model is then: a distorted ferromagnetic cone from 0 to 12 kOe; an antiferromagnetic fan from 12 to 26 kOe; a ferromagnetic fan from 26 to 56 kOe; a ferromagnet at an angle  $\theta$  that decreases with field from 56 to 300 kOe; and a ferromagnetic alignment along the  $a$  axis upwards from 300 kOe. Figures 13 and 14 (a) and 14(b) illustrate the different arrangements and the magnetization curve.

Both the magnetization data in the literature<sup>1,6</sup> and our own results (cf. Fig. 5) show an anomaly in the basal-plane magnetization at fields around 10 to 12 kOe in this temperature range. This anomaly, however, has never been pointed out, probably because it is rather small and because it does not fit with the usual description of the behavior of the cone phase when a field is applied along the  $a$  axis; our model does not provide an explanation for this anomaly either.

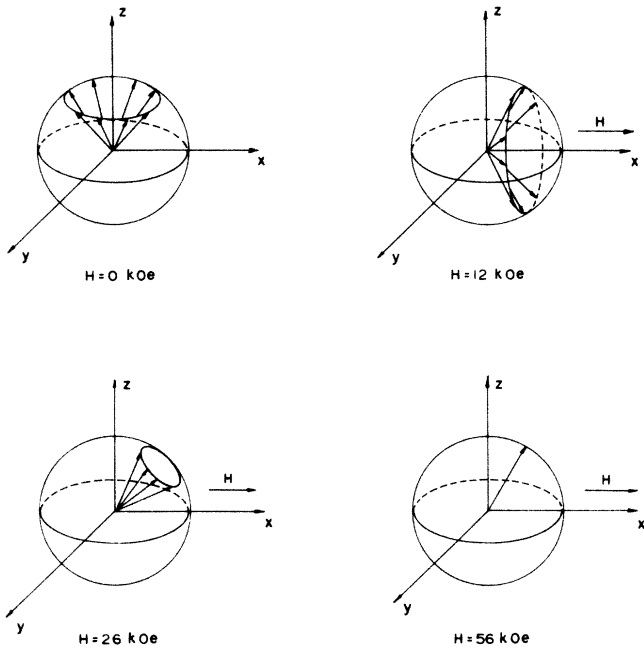


FIG. 13. Sequence of spin configurations induced by a magnetic field along the  $a$  axis for the conical phase, according to the model (see text).

In the present temperature interval the experiment shows two rather abrupt changes in the magnetization: one at 18 kOe and another at 30 kOe. Based on the theoretical work of Kitano and Nagamiya,<sup>19</sup> Coqblin<sup>1</sup> attributes the first critical field to the transition between the ferromagnetic distorted cone and the ferromagnetic fan, and the second critical field to the transition from this last arrangement into the ferromagnet at an angle  $\theta$ . The existence of this last structure above 30 kOe has been put in doubt as a consequence of the neutron diffraction experiments performed by Rhyne and Pickart,<sup>16</sup> that show a periodic arrangement of spins, compatible with the ferromagnetic fan structure, in fields up to 60 kOe.

An alternative explanation to these measurements is provided by our model. The lowest critical field (18 kOe) would be attributed to the transition from the distorted cone to the antiferromagnetic fan, which in the model occurs at 12 kOe for  $T=10$  K. The larger critical field (30 kOe) would correspond to the transition from the antiferromagnetic fan to the ferromagnetic fan, which in our model occurs at 26 kOe. This last spin arrangement would persist up to 56 kOe, when it transforms into the ferromagnet at an angle  $\theta$ . We note that in our model the transition from the distorted cone to the antiferromagnetic fan occurs with a larger change of magnetization than the transition from the antiferromagnetic fan to the ferromagnetic fan [cf. Fig. 14(b)] and that this qualitatively agrees with the experiment.<sup>1</sup> The sequence of transitions we propose agrees also with the neutron diffraction experiment of Rhyne and Pickart,<sup>6</sup> that shows that the periodic arrangement of the basal-plane components of spins persists up to 60 kOe.

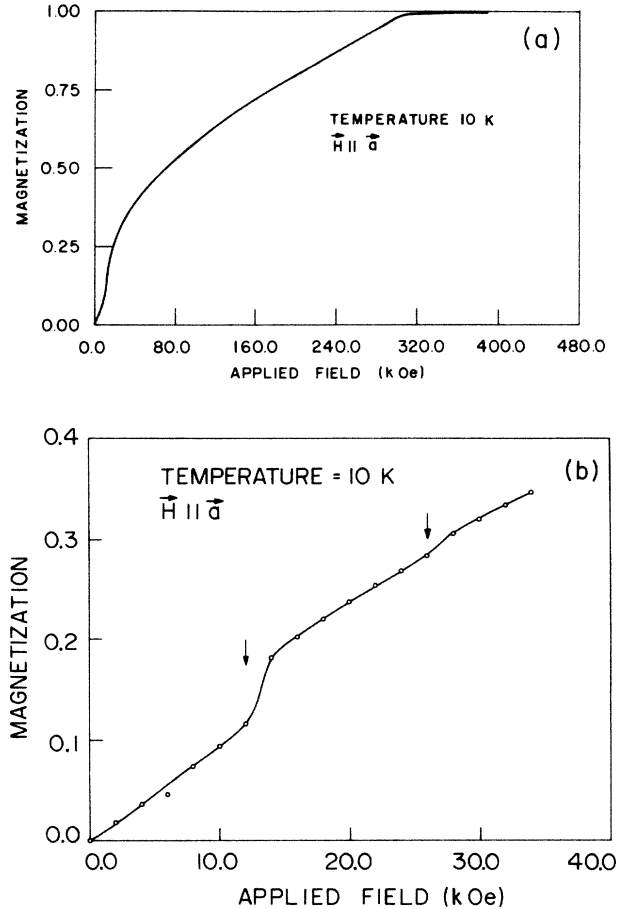


FIG. 14. (a) Magnetization curve for the sequence depicted in Fig. 13, (b) low-field part of magnetization curve shown in (a). The arrows indicate the transition fields (see text).

We should point out that the ferromagnetic alignment occurs continuously in our model and is completed at a field of 300 kOe, while the experiment shows a discontinuous transition at a field of 270 kOe (Ref. 20) (or at 150 kOe in older measurements<sup>8</sup>). It has been shown by Gibbs *et al.*<sup>3</sup> that this phase has  $\tau_m = \frac{5}{21}$ , which corresponds to a periodicity of 8.4 rather than eight layers; i.e., one would need to use a spin periodicity of 42 layers in the model to repeat precisely the experimental structure.

## 2. Field along the $c$ axis

In this case the model indicates a continuous decreasing of the cone angle  $\theta$  until, at 28 kOe, it becomes a ferromagnet along the  $c$  axis. This behavior is in accord with experiments.

## VII. SUMMARY AND CONCLUSIONS

We have performed magnetization measurements in all the ordered magnetic phases of Er, obtaining qualitative agreement with previous results.<sup>6</sup> In the conical phase it was possible to observe an anomaly when low

fields were applied in the basal plane. This anomaly is also present in the data of Feron *et al.*,<sup>6</sup> but it has not been discussed in previous publications.

We have modified a theoretical molecular-field model, first developed by Jensen,<sup>5,11</sup> by employing different values of the parameters and by introducing into the Hamiltonian an extra two-ion anisotropy term. The form of this term was chosen so that the spin-wave dispersion relations formerly obtained by Jensen<sup>11</sup> were maintained without changing the exchange parameters he proposed. To obtain a good description of the field and the temperature dependence of the magnetization, it was necessary to introduce two sets of model parameters: one for the paramagnetic and sinusoidal phases, and the other for the conical and the low-temperature antiferromagnetic phases.

Our model describes the lower-temperature antiferromagnetic phase as a helix of spins confined in a plane perpendicular to the basal plane and at 45° from the *a* axis. This structure is more symmetric than the one proposed by Jensen,<sup>5</sup> which has the spins confined to the *xz* plane. The magnetization curve obtained from our model does not present qualitative discrepancies from the experimental measurements, except that when the field is applied along the *c* axis, the model predicts a two-step transition instead of the single step observed experimentally. The field of the first step in our model coincides with that of the magnetization measurements along the *c* axis. The second step at higher fields predicted by our model can be correlated with the measured peaks in the magnetostriction and in the elastic constants  $C_{11}$  and  $C_{33}$ . In view of the recent measurements of Gibbs *et al.*,<sup>3</sup> we believe that this is a feature of our model, that forces a periodicity of eight layers rather than the 22 layers experimentally determined, and that there is only a single transition at the higher field.

For the conical phase it was necessary to include the two-ion anisotropy term to stabilize the conical structure

which, in Jensen's model, was unstable against the antiferromagnetic helix. When the field is applied in the basal plane, the model predicts a new sequence of induced structures, in which an antiferromagnetic fan appears in between the distorted cone arrangement and the ferromagnetic fan which, in Jensen's model, follows the distorted cone. The values of the calculated transition fields are only qualitatively correlated to, and somewhat smaller than, the experimental ones. One should keep in mind that our model employs the molecular-field method, and that, at low temperatures, this treatment does not describe properly the low-energy magnetic excitations of the system. As a consequence, one can only give a qualitative value to the predictions of the model, and one should not try to force a detailed description at low temperature. Nevertheless, the model suggests a different succession of structures than those predicted by the model of Jensen, and one experiment that could decide between them would be the measurement of the *c*-axis magnetization with a field applied along the *a* axis. This experiment should clearly decide whether the structure at 10 K and above 18 kOe is a distorted cone (with an appreciable *c* component) or an antiferromagnetic fan (with a zero or small *c* component). We have also discussed a possible extension that would make it possible to include in our model the spin-slip description of the magnetic structure for rational wave vectors of *c*-axis modulation.

#### ACKNOWLEDGMENTS

One of us (S.G.) would like to express his gratitude to Dr. P. L. Donoho for suggesting this field of study and for valuable orientation at the early stages of the project. He would also like to thank Dr. D. G. Pinatti for his constant encouragement along this work. Financial help from Conselho Nacional de Desenvolvimento Científico Tecnológico (CNPq) (Brazil) is also acknowledged.

- <sup>1</sup>B. Coqblin, *The Electronic Structure of Rare Earth Metals and Alloys—The Magnetic Heavy Rare Earths* (Academic, London, 1977).
- <sup>2</sup>*Handbook of Rare Earth Metals*, edited by K. A. Gschneidner, Jr. (North-Holland, Amsterdam, 1978).
- <sup>3</sup>D. Gibbs, J. Bohr, J. D. Axe, D. E. Moncton, and K. L. D'Amico, *Phys. Rev. B* **34**, 8182 (1986).
- <sup>4</sup>P. Bak, *Rep. Progr. Phys.* **45**, 588 (1982). In this review article the type of ideas that lead to the concept of spin discommensurations are discussed within mean-field theory.
- <sup>5</sup>J. Jensen, *J. Phys. F* **6**, 1145 (1976).
- <sup>6</sup>J. L. Feron, G. Hug, and R. Pauthenet, *Z. Angew. Phys.* **30**, 61 (1970).
- <sup>7</sup>See article by K. A. McEwen, in *Handbook of Rare Earth Metals*, edited by K. A. Gschneidner, Jr. (North-Holland, Amsterdam, 1978), Vol. 1, p. 427.
- <sup>8</sup>J. J. Rhyne, S. Foner, B. J. McNiff, and R. J. Doelo, *J. Appl. Phys.* **39**, 892 (1968).
- <sup>9</sup>R. B. Flippen, *J. Appl. Phys.* **35**, 1047 (1964).
- <sup>10</sup>R. M. Nicklow, N. Wakabayashi, M. K. Wilkinson, and R. E. Reed, *Phys. Rev. Lett.* **27**, 334 (1971).
- <sup>11</sup>J. Jensen, *J. Phys. F* **4**, 1065 (1974).

- <sup>12</sup>P. A. Lindgard and O. Danielson, *J. Phys. C* **7**, 1523 (1974).
- <sup>13</sup>In our calculations we had to change the sign of the crystal-field parameter  $B_{40}$  given by Jensen (Ref. 5) because we could not otherwise obtain the conical arrangement of spins. We believe that this is a typographical error in this paper.
- <sup>14</sup>J. W. Cable, B. I. Wollan, W. C. Koehler, and M. K. Wilkinson, *Phys. Rev.* **140**, A1896 (1965).
- <sup>15</sup>M. Habenschuss, C. Stassis, S. K. Sinha, H. W. Deckman, and F. H. Spedding, *Phys. Rev. B* **10**, 1020 (1974).
- <sup>16</sup>J. J. Rhyne and S. J. Pickart, *Magnetism and Magnetic Materials—1971, Chicago*, Proceedings of the 17th Annual Conference on Magnetism and Magnetic Materials, AIP Conf. Proc. No. 5, edited by D. C. Graham and J. J. Rhyne (AIP, New York, 1972).
- <sup>17</sup>J. J. Rhyne and S. Legvold, *Phys. Rev.* **140**, A2143 (1965).
- <sup>18</sup>D. C. Giles and S. B. Palmer, *J. Appl. Phys.* **52**, 1113 (1981).
- <sup>19</sup>Y. Kitano and T. Nagamiya, *Progr. Theor. Phys.* **31**, 1 (1964).
- <sup>20</sup>V. L. Yakovenko, V. E. Bril, V. V. Druzhininin, R. Z. Levitin, V. M. Mel'nikov, and R. B. Ozipova, *Zh. Eksp. Teor. Fiz.* **78**, 157 (1980) [*Sov. Phys.—JETP* **51**, 77 (1980)].